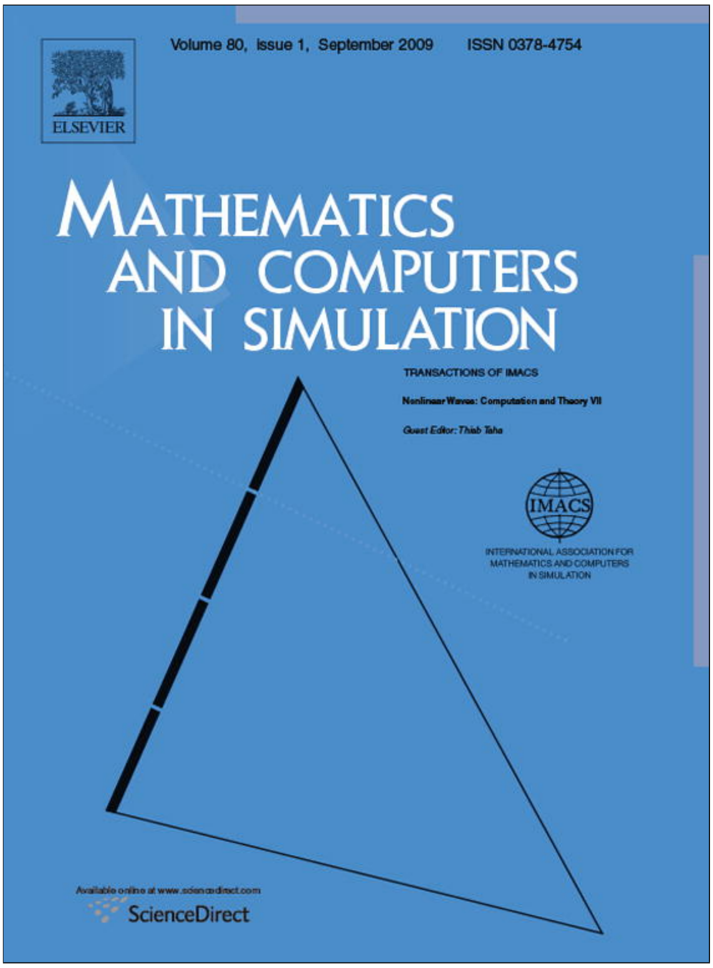
Volume 80, Issue 1, September 2009 ISSN 0378-4754
ELSEVIER
MATHEMATICS AND COMPUTERS IN SIMULATION
TRANSACTIONS OF IMACS
Nonlinear Waves: Computation and Theory VII
Guest Editor: Thiab Taha
IMACS
INTERNATIONAL ASSOCIATION FOR MATHEMATICS AND COMPUTERS IN SIMULATION
Available online at www.sciencedirect.com
ScienceDirect

Available online at www.sciencedirect.com
ScienceDirect
Mathematics and Computers in Simulation 80 (2009) 46–55
MATHEMATICS AND COMPUTERS IN SIMULATION
www.elsevier.com/locate/matcom

# Impact of the large cross-modulation parameter on the collision dynamics of quasi-particles governed by vector NLSE

M.D. Todorov [a], C.I. Christov [b,∗]

[a] Dept of Diff. Equations, Faculty of Applied Math. and Informatics, Technical University of Sofia, Sofia, 1000, Bulgaria
[b] Dept of Mathematics, University of Louisiana at Lafayette, LA 70504-1010, USA

Available online 18 June 2009

**Abstract**

For the Coupled Nonlinear Schrödinger Equations (CNLSE) we construct a conservative fully implicit scheme (in the vein of the scheme with internal iterations proposed in [C.I. Christov, S. Dost, G.A. Maugin, Inelasticity of soliton collisions in system of coupled nls equations, Physica Scripta 50 (1994) 449–454.]). Our scheme makes use of complex arithmetic which allows us to reduce the computational time fourfold. The scheme conserves the "mass", momentum, and energy.

We investigate collisions of solitary waves (quasi-particles or QPs) with linear polarization in the initial configuration. We elucidate numerically the role of nonlinear coupling on the quasi-particle dynamics. We find that the initially linear polarizations of the QPs change after the collision to elliptic polarizations. For large values of cross-modulation parameter, an additional QP is created during the collision. We find that although the total energy is positive and conserved, the energy only of the system of identifiable after the collision QPs is negative, i.e., the different smaller excitations and radiation carry away part of the energy. The effects found in the present work shed light on the intimate mechanisms of interaction of QPs.


*PACS:* 02.70.-c; 05.45.Yv; 42.65.Tg

*Keywords:* Coupled Nonlinear Schrödinger Equations (CNLSE); Cross-modulation; Quasi-particles

## 1. Introduction

The investigation of soliton supporting systems is of great importance both for the applications and for the fundamental understanding of the phenomena associated with propagation of solitons. Apart from its crucial importance in optics, the Nonlinear Schrödinger Equation (NLSE) is a nonlinear dispersive equation on its own right in which the nonlinearity and dispersion can be balanced allowing localized structures to propagate without change.

Recently, elaborate models such as Coupled Nonlinear Schrödinger Equations (CNLSE) appeared in the literature (see the extensive survey [11] and the literature cited therein). They involve more parameters and have richer phenomenology but, as a rule, are not fully integrable and require numerical approaches. The nonfully integrable models possess three conservation laws: for (wave) "mass", (wave) momentum, and energy and these have to be faithfully represented by the numerical scheme.

An implicit scheme of Crank–Nicolson type was first proposed for the single NLS in the extensive numerical treatise [14]. The concept of the internal iterations was applied to CNLSE in [6] and extended in [12] in order to ensure the

∗ Corresponding author. Tel.: +1 337 482 5273; fax: +1 337 482 5346.
*E-mail address:* christov@louisiana.edu (C.I. Christov).

0378-4754/$36.00 © 2009 IMACS. Published by Elsevier B.V. All rights reserved.
doi:10.1016/j.matcom.2009.06.020

implementation of the conservation laws on difference level within the round-off error of the calculations. The CNLSE is investigated numerically also in [8]. Here, we follow generally the works [6,12] but focus on a new complex-variable implementation of the conservative scheme. This allows us to invert (albeit complex-valued) matrices which have just five diagonals, while the real-valued scheme requires the inversion of nine-diagonal matrices [6,12]. To this end, we generalize the computer code for Gaussian elimination with pivoting developed earlier for real-valued algebraic systems in [5]. This gives a significant advantage in the efficiency of the algorithm. The numerical validation of the new code includes comparisons with [6,12] which show that the complex-number implementation of the scheme gives identical results with the real-number codes but is approximately four times as efficient.

The aim of our work is to understand better the particle-like behavior of the localized waves. We call a localized wave a quasi-particle (QP) if it survives the collision with other QPs (or some other kind of interactions) without losing its identity.

## 2. Coupled Nonlinear Schrödinger Equations

In optics, the most popular model is the cubic Schrödinger equation which describes the single-mode wave propagation in a fiber [2]. A general form of the Coupled Nonlinear Schrödinger Equations (CNLSE) reads

$$\mathrm{i}\psi_t = \beta\psi_{xx} + [\alpha_1|\psi|^2 + (\alpha_1 + 2\alpha_2)|\phi|^2]\psi + \gamma\psi + \Gamma\phi, \tag{1}$$

$$\mathrm{i}\phi_t = \beta\phi_{xx} + [\alpha_1|\phi|^2 + (\alpha_1 + 2\alpha_2)|\psi|^2]\phi + \gamma\phi + \Gamma\psi, \tag{2}$$

where $\beta$ is the dispersion coefficient and $\alpha_1$ describes the self-focusing of a signal for pulses in birefringent media. Complex-valued coefficients $\gamma$ and $\Gamma$ are responsible for the linear coupling between the two equations. Respectively $\alpha_2$ governs the nonlinear coupling between the equations. It is interesting to note that despite the fact that "cross-terms" proportional to $\alpha_1$ appear in the equations, a nonlinear coupling for $\alpha_2 = 0$ is absent because the solution of the two equations are identical, $\psi \equiv \phi$, and equal to the solution of a single NLSE. In this instance we refer the reader to Manakov [10] who generalized an earlier result by Zakharov and Shabat [17,18] for the scalar cubic NLSE. We will refer in the present work to $\alpha_2$ as a cross-modulation parameter (see also [7]) because when $\alpha_2 \neq 0$ one actually gets interaction between the two components. In fact $\alpha_2$ plays an important role in defining the elliptic, circular and linear polarizations. In the case $\alpha_2 \neq 0$, the integrability is lost, and numerical methods are to be used.

Functions $\psi$ and $\phi$ have various interpretations in the context of optic pulses including the amplitudes of $x$ and $y$ polarizations in a birefringent nonlinear planar waveguide, pulsed wave amplitudes of left and right circular polarizations, etc. The quantity $\gamma$ is called normalized birefringence, and $\Gamma$ is the relative propagation constant. The presence of the two new parameters, $\gamma$ and $\Gamma$, makes the phenomenology of the system much richer. In particular, they allow to study the phenomena such as "self-dispersion", "cross-dispersion", and dissipation, etc. (see [12] and the literature cited therein).

For $\Gamma = \gamma = 0$, Eqs. (1) and (2) are alternatively called the Gross–Pitaevskii equations or a system of Manakov type. As already mentioned, it can be solved analytically for $\alpha_2 = 0$. We derive the pertinent theoretical and numerical formulas for the general case, but focus our attention on the case $\Gamma = \gamma = 0$ in the actual numerical experiments.

## 3. Conservation laws and Hamiltonian structure of CNLSE

It is very important for the quasi-particle approach to have the Hamiltonian structure of the system under consideration. Curiously enough, we were unable to find papers in the literature that address systematically these issues. The Hamiltonian for a single NLSE can be found in [4] (see also the monographs [1,3]). For CNLSE, some limited version of the Lagrangian is given in [16], but no full-fledged Lagrangian is available in the literature. For this reason, we begin with the following The Lagrangian of the CNLSE system Eqs. (1) and (2) is given by

$$L \stackrel{\mathrm{def}}{=} \frac{\mathrm{i}}{2}(\psi_t\bar{\psi} - \bar{\psi}_t\psi) + \frac{\mathrm{i}}{2}(\phi_t\bar{\phi} - \bar{\phi}_t\phi) - \beta(|\psi_x|^2 + |\phi_x|) + \frac{\alpha_1}{2}(|\psi|^4 + |\phi|^4)$$
$$+(\alpha_1 + 2\alpha_2)|\psi|^2|\phi|^2 + \gamma(|\psi|^2 + |\phi|^2) + 2\Gamma[\Re(\bar{\psi}\bar{\phi})]. \tag{3}$$

**Proof.** Direct inspection shows that the Euler–Lagrange equations (E-L) for the conjugated functions $\bar\psi$ and $\bar\phi$ give the original Eqs. (1) and (2), while E-L for the functions $\psi$ and $\phi$ give the conjugated system.

$$-\mathrm{i}\bar\psi_t = \beta\bar\psi_{xx} + [\alpha_1|\psi|^2 + (\alpha_1+2\alpha_2)|\phi|^2]\bar\psi + \gamma\bar\psi + \Gamma\bar\phi \tag{4}$$

$$-\mathrm{i}\bar\phi_t = \beta\bar\phi_{xx} + [\alpha_1|\phi|^2 + (\alpha_1+2\alpha_2)|\psi|^2]\bar\phi + \gamma\bar\phi + \Gamma\bar\psi. \tag{5}$$

Now the Hamiltonian is defined via the Legendre transformation

$$H = \frac{\partial L}{\partial \psi_t}\psi_t + \frac{\partial L}{\partial \bar\psi_t}\bar\psi_t + \frac{\partial L}{\partial \phi_t}\phi_t + \frac{\partial L}{\partial \bar\phi_t}\bar\phi_t - L = \beta(|\psi_x|^2 + |\phi_x|^2) - \frac{\alpha_1}{2}(|\psi|^4 + |\phi|^4)$$
$$-(\alpha_1+2\alpha_2)|\psi|^2|\phi|^2 - \gamma(|\psi|^2+|\phi|^2) - 2\Gamma[\Re(\bar\psi\bar\phi)]. \tag{6}$$

On the interval $x \in [L_1, L_2]$ we impose trivial b.c. for the functions $\psi$,$\phi$ and evaluate the integral of the following

$$\bar\psi_t \cdot \text{Eq. (1)} + \psi_t \cdot \text{Eq. (4)} + \bar\phi_t \cdot \text{Eq. (2)} + \phi_t \cdot \text{Eq. (5)}$$

After some tedious but straightforward derivations in which the asymptotic boundary conditions are acknowledged, we obtain the conservation law for the energy

$$\frac{d}{dt}\int_{L_1}^{L_2}[-\beta(|\psi_x|^2+|\phi_x|^2) + \frac{\alpha_1}{2}(|\psi|^4+|\phi|^4) + (\alpha_1+2\alpha_2)|\psi|^2|\phi|^2 + \gamma(|\psi|^2+|\phi|^2 + 2\Gamma[\Re(\bar\psi\bar\phi)]]dx) = 0. \tag{7}$$

Since the integrand in Eq. (7) is $-H$, it proves that the Hamiltonian dose represents the energy density for this system. For the wave momentum we have the definition

$$P = \int_{L_1}^{L_2}\frac{i}{2}[(\psi\bar\psi_x - \psi_x\bar\psi) + (\phi\bar\phi_x - \phi_x\bar\phi)]dV = -\int_{L_1}^{L_2}\Im[\psi\bar\psi_x + \phi\bar\phi_x]dx. \tag{8}$$

Similarly to the derivations for the energy, we consider

$$\bar\psi_x \cdot \text{Eq. (1)} + \psi_x \cdot \text{Eq. (4)} + \bar\phi_x \cdot \text{Eq. (2)} + \phi_x \cdot \text{Eq. (5)} \tag{9}$$

and after some algebra we get

$$\frac{\mathrm{d}P}{\mathrm{d}t} = \int_{L_1}^{L_2}\frac{d}{dx}\{\beta(|\psi_x|^2+|\phi_x|^2) - \frac{\alpha_1}{2}(|\psi|^4+|\phi|^4) - (\alpha_1+2\alpha_2)|\psi|^2|\phi|^2$$
$$-\gamma(|\psi|^2+|\phi|^2) - 2\Gamma[\Re(\bar\psi\bar\phi)]\}dx = H|_{L_1}^{L_2}, \tag{10}$$

which is the balance law for the wave momentum. For asymptotic b.c. this balance law becomes a conservation law. Note that in higher dimensions the wave momentum is a vector and in establishing Eq. (10), the divergence theorem has to be used. Note that in the case of asymptotic b.c., i.e., when $|L_1|,|L_2| \to \infty$, the balance law for the momentum, Eq. (10), becomes a conservation law as well.

In the end we take the integral of the combination

$$\bar\psi_t \cdot \text{Eq. (1)} - \psi_t \cdot \text{Eq. (4)} + \bar\phi_t \cdot \text{Eq. (2)} - \phi_t \cdot \text{Eq. (5)} \tag{11}$$

which gives us the conservation of "mass"

$$\frac{dM}{dt} = 0, \qquad M \equiv \int_{L_1}^{L_2}(|\psi|^2+|\phi|^2)dx. \tag{12}$$

## 4. Conservative difference scheme in complex arithmetic

For the sake of selfcontainedness of the present paper we briefly discuss here the scheme developed in [15]. Consider a uniform mesh in the interval $[L_1, L_2]$,

$$x_i = (i-1)h, \qquad h = \frac{L_2 - L_1}{N-1} \quad \text{and} \quad t^n = n\tau,$$

where $N$ is the total number of grid points in the interval and $\tau$ is the time increment. Respectively, $\psi_i^n$ and $\phi_i^n$ denote the value of the $\psi$ and $\phi$ at the $i$th spatial point and time stage $t^n$. Clearly, $n = 0$ refers to the initial conditions.

Our purpose is to create a difference scheme that is not only convergent (consistent and stable), but also reflects the conservation laws. A scheme that satisfies those requirements reads

$$\begin{aligned} \mathrm{i}\frac{\psi_i^{n+1} - \psi_i^n}{\tau} &= \frac{\beta}{2h^2}(\psi_{i-1}^{n+1} - 2\psi_i^{n+1} + \psi_{i+1}^{n+1} + \psi_{i-1}^n - 2\psi_i^n + \psi_{i+1}^n) + \frac{\gamma}{2}(\psi_i^n + \psi_i^{n+1}) \\ &+ \frac{\Gamma}{2}(\phi_i^n + \phi_i^{n+1}) + \frac{\psi_i^{n+1} + \psi_i^n}{4}[\alpha_1(|\psi_i^{n+1}|^2 + |\psi_i^n|^2) + (\alpha_1 + 2\alpha_2)(|\phi_i^{n+1}|^2 |\phi_i^n|^2)] \end{aligned} \tag{13}$$

$$\begin{aligned} \mathrm{i}\frac{\phi_i^{n+1} - \phi_i^n}{\tau} &= \frac{\beta}{2h^2}(\phi_{i-1}^{n+1} - 2\phi_i^{n+1} + \phi_{i+1}^{n+1} + \phi_{i-1}^n - 2\phi_i^n + \phi_{i+1}^n) + \frac{\gamma}{2}(\phi_i^n + \phi_i^{n+1}) + \frac{\Gamma}{2}(\psi_i^n + \psi_i^{n+1}) \\ &+ \frac{\phi_i^{n+1} + \phi_i^n}{4}[\alpha_1(|\phi_i^{n+1}|^2 + |\phi_i^n|^2) + (\alpha_1 + 2\alpha_2)(|\psi_i^{n+1}|^2 + |\psi_i^n|^2)]. \end{aligned} \tag{14}$$

In Ref. [6], it was proved that the scheme Eqs. (13) and (14) conserves the discrete analogs of mass and energy, namely, for all $n \geq 0$, we have

$$M^n = \sum_{i=2}^{N-1}(|\psi_i^n|^2 + |\phi_i^n|^2) = \text{const}, \qquad E^n = \sum_{i=2}^{N-1}\frac{\beta}{2h^2}(|\psi_{i+1}^n - \psi_i^n|^2 + |\phi_{i+1}^n - \phi_i^n|^2) - \frac{\alpha_1}{4}(|\psi_i^n|^4 + |\phi_i^n|^4)$$

$$-\frac{\alpha_1 + 2\alpha_2}{2}(|\psi_i^n|^2|\phi_i^n|^2) - \frac{\gamma_r^\phi}{2}|\phi_i^n|^2 - \frac{\gamma_r^\psi}{2}|\psi_i^n|^2 - \Gamma\Re[\overline{\phi}_i^n\psi_i^n] = \text{const}.$$

The discrete balance law for the momentum is also faithfully represented.

The scheme Eqs. (13) and (14) cannot be implemented directly, because it is nonlinear with respect to the variables $\psi_i^{n+1}$ and $\phi_i^{n+1}$. Internal iterations are introduced in the fashion of [6,12,15] and for the current iteration of the unknown functions (superscript $n+1$, $k+1$) we have an implicitly coupled system of two tridiagonal systems with complex coefficients. In order to be solved, this system is recast as a single five-diagonal system. For the inversion of the five-diagonal $2N \times 2N$ matrix we created an algorithm based on Gaussian elimination with pivoting which is a generalization of a similar algorithm [5] for a real-valued system. As it should have been expected, the computational time needed to complete the calculations for a given set of parameters is four times shorter for the scheme with complex arithmetic than for the scheme with real arithmetic.

It is to be noted here, that for the cubic nonlinearity under consideration, one can create a scheme that is not nonlinearly coupled but such a scheme cannot be generalized for other type of nonlinearities.

We conduct the internal iterations (repeating the calculations for the same time step $(n+1)$ with increasing value of the superscript $k$) until convergence, i.e., when both the following criteria are satisfied

$$\max_i|\{\psi,\phi\}_i^{n+1,k+1} - \{\psi,\phi\}_i^{n+1,k}| \leq 10^{-12}\max_i|\{\psi,\phi\}_i^{n+1,k+1}|. \tag{15}$$

After the internal iterations converge, one gets $\psi^{n+1} \equiv \psi^{n+1,k+1}$ and $\phi^{n+1} \equiv \phi^{n+1,k+1}$ which are the solutions of the nonlinear implicit scheme, Eqs. (13) and (14). We mention here that for physically reasonable time increments $\tau$ the number of internal iterations needed for convergence is four to six, which is a small price to pay to have fully implicit, nonlinear and conservative scheme.

The scheme has been thoroughly validated through the standard numerical tests involving doubling/halving the spacing and time increment. The results confirm the second order of accuracy in space and time. Another crucial validation has been made by a direct comparison with the results [6,12]. We did repeat a couple of the more difficult cases using both the scheme with real arithmetic and the presented here scheme with complex arithmetic. The results with the same scheme parameters turn out to indistinguishable within the order of round-off error.

## 5. Interaction of Solitons: numerical results

CNLSE possess solutions that are localized envelopes. Since CNLSE is a two-component system, generally speaking the envelops for each $\psi$,$\phi$ can have different amplitudes. In addition, the carrier frequency for each component can be different. This brings into view the notion of polarization which reflects the relative importance of the two components. The most general polarization is the elliptic one (see, e.g., [13]) but no analytical expression is available for the solution. As initial condition we consider the case of a particular linear polarization when one of the components is not present. For instance, when $\psi = 0$ or $\phi = 0$ we stipulate that the respective $\psi$- or $\phi$-profile is given by

$$\psi(x,t), \phi(x,t) = A_{\psi,\phi}\mathrm{sech}[b_{\psi,\phi}(x - X - \mathrm{ct})]\exp\left\{\mathrm{i}\left[\frac{c}{2\beta}(x - X - ct) - n_{\psi,\phi}t\right]\right\}. \tag{16}$$

and it is easy to show that the parameters for which such solution is possible are

$$b^2_{\psi,\phi} = \frac{1}{\beta}\left(n_{\psi,\phi} + \frac{c^2}{4\beta}\right), \qquad A_\psi = b_\psi\sqrt{\frac{2\beta}{\alpha_1}}, \qquad u_c = \frac{2n_{\psi,\phi}\beta}{c},$$

which means that for given phase speed, $c$, and carrier frequencies, $n_\psi$,$n_\phi$, the solution of the above type is fully specified. The localized solution is identified by the presence of a special point, $x = X - \mathrm{ct}$ ("center") which moves with a given phase speed $c$. The center is common for both components $\psi$ and $\phi$.

For consistency, we keep the grid parameters fixed and the values of the initial phase speeds are selected to be $c_{\mathrm{left}} = 1$, $c_{\mathrm{right}} = -0.5$. We began with the case $\alpha_2 = 0$ and confirmed that there was no interaction between the two initially orthogonal pulses. The interaction becomes appreciable around $\alpha_2 = 0$ when the smaller QP becomes elliptically polarized (see the upper panel of Fig. 1). The transformation of pulses after collision was reported in [[9], Fig. 3] but no systematic numerical experiments are available in the literature about the change of polarization as a result of the integration. In addition, because of the interaction the larger QP is slightly accelerated, while the smaller QP is slowed

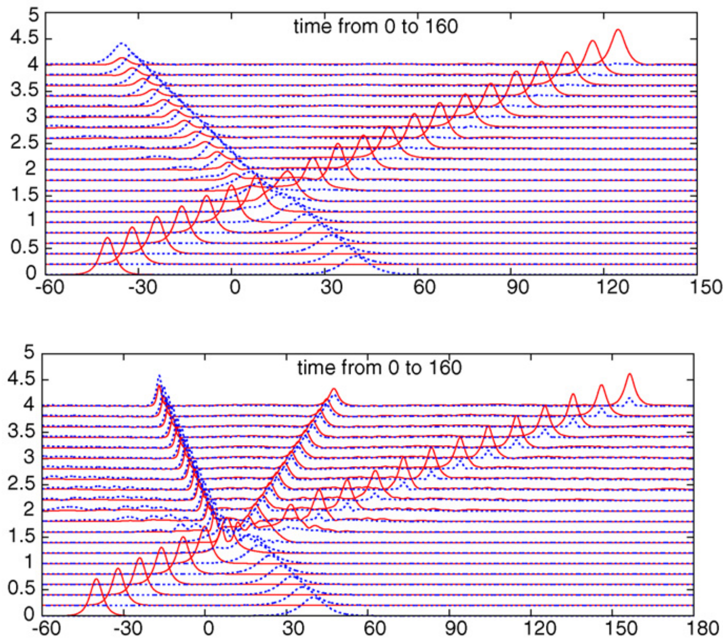


Fig. 1. Head-on collision for $c_{\mathrm{left}} = 1$, $c_{\mathrm{right}} = -0.5$. Solid line: $|\psi|$; dashed line: $|\phi|$. Upper panel: $\alpha_2 = 2$, and lower panel: $\alpha_2 = 6$.

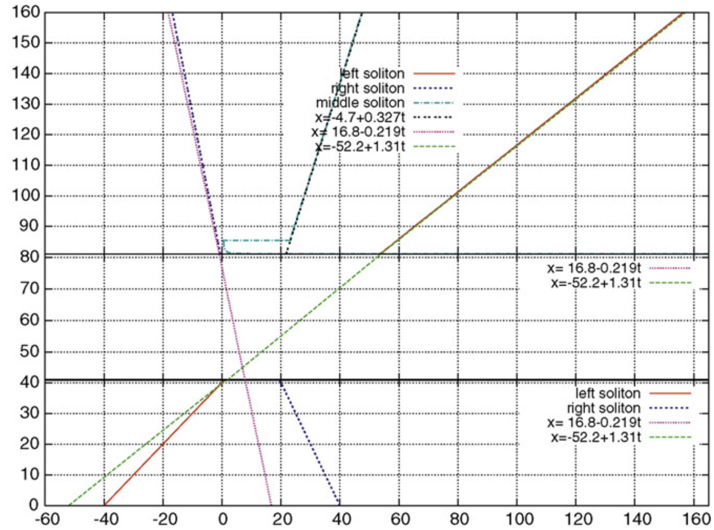


Fig. 2. Trajectories of the quasi-particles for $\alpha_2 = 6$. Horizontal axis is $x$.

down. Increasing the cross-modulation to $\alpha_2 = 4$ does not change qualitatively the above described dynamics of QP. The difference from the case $\alpha_2 = 2$ is mostly in the increased amplitude of the excited orthogonal modes of the solitons, especially the $\psi$-soliton accompanying the smaller left-going $\phi$ soliton. The support of the left-going QP becomes shorter, and the QP slows further down while the larger (right-going) QP is even more accelerated.

The qualitative change of the dynamics is observed around. As shown in the lower panel of Fig. 1, apart from the increased amplitudes of the excited accompanying components, a third QP appears as a result of the interaction. There was some small hint at this effect even for smaller $\alpha_2 = 4$, but now it is more pronounced. It is interesting that the third QP is moving to the right and its birth does not seem to slow the right-going QP. In fact, the latter acquires even faster phase speed. The trajectories of the centers of QPs are presented in see Fig. 2. The kinetic energy of the larger QP increases after the interaction while the internal energy of the smaller particle decreases so much that it becomes negative (to a smaller extent this effect is observed also for the weak interaction, $\alpha_2 = 2$). In a sense, the internal energy of the smaller QP is converted to the kinetic energy of the larger particle and is also used to create a new QP between the two main QPs. We can call this "recoil effect".

To understand better the mechanism of interaction, we investigate the motion of a QPs in their moving frames. To this end we track the center of the QP assuming that it is the point of maximum of the modulo of the larger component. Then we find the time dependence of $\psi$ and $\phi$ in the point of the said maximum. As a result we get periodic functions of time whose periods give the carrier frequencies in the moving frame. The change of the carrier frequency in the wake of the interaction is depicted in Fig. 3 where only the left-going QP is considered. The situation with the right-going particle is qualitatively similar, but there are quantitative differences. For instance, the carrier frequency of the excited $\phi$-component for the right-going QP is much higher. The relevant graph is not presented here in order not to overload the text.

It is interesting to note here that for the newborn QP (see the lower panel of Fig. 1), the amplitudes of the $\psi$- and $\phi$-components are commensurate but the carrier frequency of the latter is much higher, which means that it is not circularly polarized with angle close to 45° but is, in fact, an elliptically polarized solution. The third QP has somewhat larger support than the left-going one.

We found the best-fit of formulas of type of Eq. (16) to the profiles after the interaction in order to extract the pure QPs from the field after the interaction. Although in the case of elliptic polarization, the solution is not strictly a sec $h$, it is still close enough in order to make this kind of extraction worthwhile. Fig. 4 shows the results. The panel (a) presents the $\psi$- component of the large (right-going) QP. Since the $\phi$ component is not very large, we do not present it in the figure. Clearly, the deformation of the larger QP is not very strong. The panels (b) and (c) present the components of the smaller (left-going) QP after the collision. The excited signal is commensurate with the main component. A similar situation is observed for the newborn QP in panels (d) and (e). The estimated best-fit parameters can be used to compute analytically the energies and momenta of the different QPs.

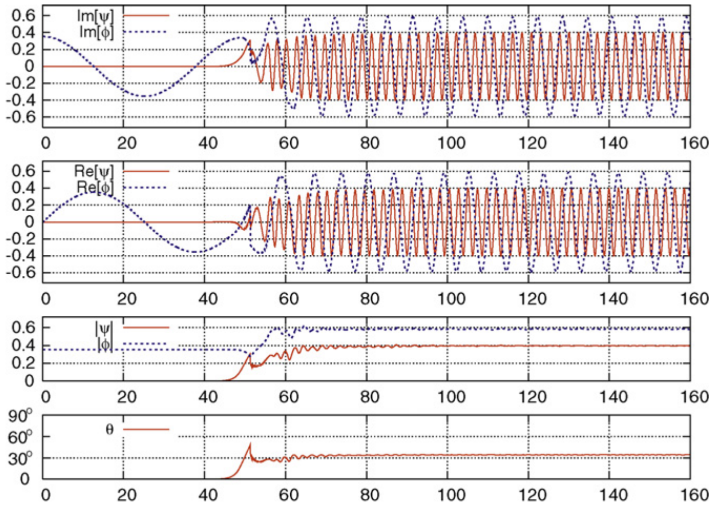


Fig. 3. Temporal behavior of the left-going QP in its moving frame for $\alpha_2 = 6$. Horizontal axis is the time, $t$.

One can see in Table 1 that the energy of the left-going QP is negative, $E = -0.4020$ as computed on the basis of the best-fit parameters. This raises the question of the reliability of the result. In order to verify the latter, we clipped the region around the left-going QP and computed numerically the energy and the other characteristics directly from the available profile. We have found that the directly evaluated energy over the truncated interval is $E = -0.3878$ which

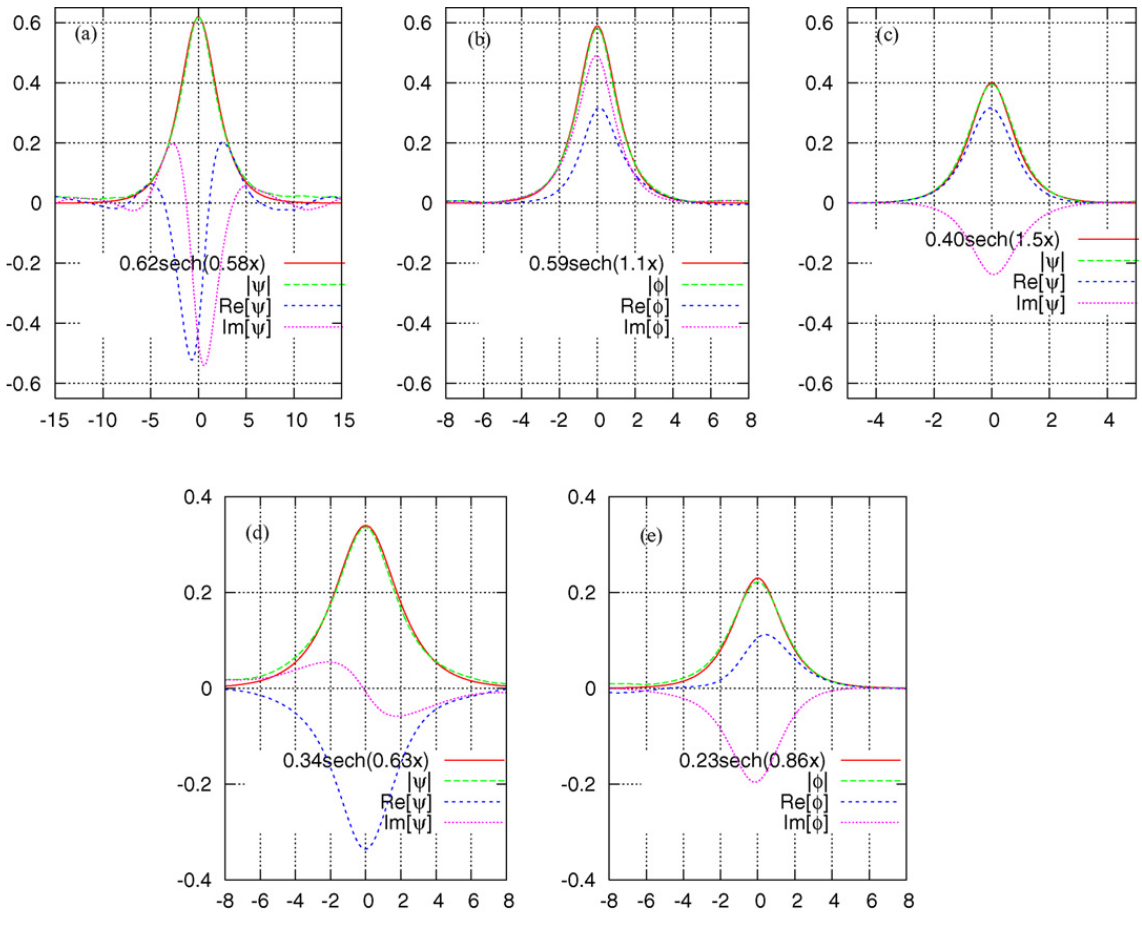


Fig. 4. Best-fit approximations of sec $h$ type to the modulo of $\psi$ and $\phi$ for $c_l = 1$, $c_r = -0.5$, $\alpha_2 = 6$. (a): $\psi$ component of the right-going QP; (b), (c): $\phi$- and $\psi$-components of the left-going QP; (d), (e) $\psi$- and $\phi$-component of the newborn QP. The horizontal axis is $x - X(t)$, where $X(t)$ is the center of the respective QP.

Table 1
Properties of quasi-particles (QPs) for $c_l = 1$, $c_r = -0.5$, and $\alpha_2 = 6$ before and after the collision.

| Soliton | $M$ | $c$ | $E_k$ | $E_p$ | $E$ | $P$ |
|---|---|---|---|---|---|---|
| Before collision | | | | | | |
| Left (right-going) | 1.0 | 1.0 | 0.5000 | −0.1667 | 0.3333 | 1.00 |
| Right (left-going) | 0.5 | −0.5 | 0.0625 | −0.0208 | 0.0417 | −0.25 |
| Total | 1.5 | 0.5[a] | 0.5625 | −0.1875 | 0.3750 | 0.75 |
| After collision | | | | | | |
| Right (right-going) | 0.6830 | 1.31 | 0.5861 | −0.1848 | 0.4013 | 0.8948 |
| Left (left-going) | 0.4231 | −0.219 | 0.0102 | −0.4122 | −0.4020 | −0.0927 |
| Middle (newborn) | 0.2450 | 0.327 | 0.0131 | −0.0797 | −0.0666 | 0.0801 |
| Total | 1.3512 | 0.6529[†] | 0.6093 | −0.6767 | −0.0673 | 0.8822 |

[a] The speed of the center of mass $c = P_{\text{total}}/M_{\text{total}}$.

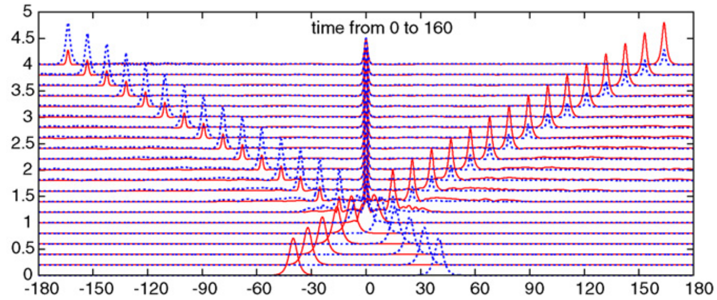


Fig. 5. Collision of two equal QPs for $\alpha_2 = 6$, $c_l = c_r = 1$.

confirms the validity of the best-fit formulas. Respectively, for the directly computed mass we got $M = 0.413$ which is in very good agreement with the best-fir result of 0.4231 (see the respective entry of Table 1).

A natural question arises here about the symmetry of the interaction, when the initial configuration of the solitons is perfectly symmetric. To investigate this we conducted a numerical experiment with two QPs with equal initial phase speeds, $c_l = c_r = 1$. The expectation is that the third QP will stay in the origin of the coordinate system, i.e., a standing soliton should be born. Indeed, Fig. 5 shows that our computations confirmed this supposition. The two main QPs evolve perfectly symmetric after the collision and the newborn QP is a standing soliton. Note that the amplitudes of the two components of the standing soliton appear to be equal to each other. A close examination of their carrier frequencies shows that in fact they are also equal which means that the standing soliton has circular polarization with angle $\theta = 45^\circ$. The masses, energies and momenta of the QPs in the symmetric case are qualitatively similar to the case $c_l = 1$, $c_r = -0.5$ and will not be presented here.

In the end we consider also the case $\alpha_2 = 10$ when the cross-modulation becomes a very strong effect. Fig. 6 shows the further increase in the excitability of the system. The main difference from $\alpha_2 = 6$ is that the left-going QP splits into two very narrow QPs which are moving with much faster phase speeds than the original left-going QP. In addition, the right-going QP also gets its support shortened. Another very important trait of the interaction for this very large $\alpha_2 = 10$ is the appearance of considerable radiation that carries away the kinetic energy of the system and the total

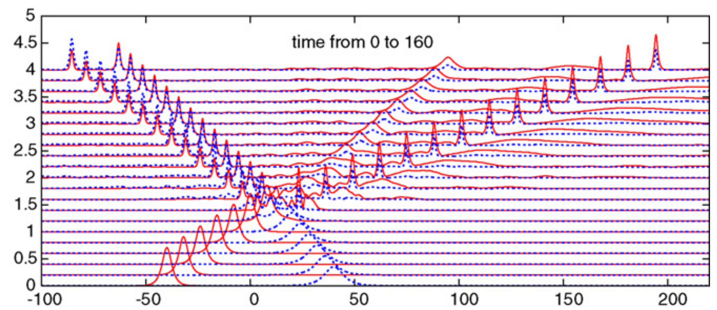


Fig. 6. Collision of two equal QPs for $\alpha_2 = 10$, $c_l = 1$, $c_r = -0.5$.

Table 2
Integral characteristics of excitations.

| | Left forerunner | Between QP-2 and QP-3 | Between QP-3 and QP-4 | Right forerunner |
|---|---|---|---|---|
| $M$ | 0.0431 | 0.0269 | 0.05908 | 0.1969 |
| $P$ | 0.0082 | 0.0083 | 0.07669 | 0.4087 |
| $E$ | 0.2215 | 0.0044 | 0.0045 | 0.7225 |

energy of the QPs is radically different from the total energy of the initial wave profile. The differences are so drastic that the sum of QPs energies can even become negative. This means that the energy was carried away by the radiation.

In order to confirm this conjecture we consider the final time stage from Fig. 6, clip away the main QPs and calculate the energy of the wave profile that is left in the reduced region. As one can see, the amplitude of the radiation that dwells in the mentioned region is rather small. Yet the energy of the oscillations is very large, particularly, the kinetic energy. We enumerate the different QPs from left to right, namely the leftmost soliton is QP-1, and the rightmost is QP-4. The results are organized in Table 2 for the different regions, save the small interval between QP-1 and QP-2 whose characteristics are negligible.

The masses and the pseudomomenta of the excitations are commensurate with their relative importance for the amplitudes of the total wave profile. The predominant part of the kinetic energy is concentrated in the left and right forerunners because they propagate with very large phase speeds, and span large portions of the region.

Finally, we add together the energies of all four QPs and the excitations alike and get results which are within 20% of the total energy as conserved of the scheme. This means that the large negative energies of the QPs are the result of the evacuation of energy by the forerunners and is not a numerical effect. This kind of transformation is a physical effect that is connected with the excitability of the system and is not present in the case of a single Schrödinger equation.

## 6. Conclusion

In this paper we develop a complex-arithmetic implementation of a conservative difference scheme for Coupled Nonlinear Schrödinger Equations (CNLSE). To this end a special solver for Gaussian elimination with pivoting is developed for multi-diagonal complex-valued matrices, which is a generalization of the solver created earlier by one of the authors. The new solver allows us to use grids of considerable sizes (up to 20,000 grid points) and small time increments obtaining thus a reliable approximation.

The algorithm is validated by the mandatory numerical tests involving doubling the mesh size and halving the time increment, as well as by the direct comparison with the real-arithmetic schemes [6,12]. The advantages of the new scheme are that the band of the matrix is twice smaller and that the overall number of unknowns is also twice smaller. Our numerical tests show that, as expected, it performs four times faster than the scheme from [6,12].

The new tool developed here allowed us to consider physically important sets of parameters of the CNLSE and to investigate the role of nonlinear coupling in the quasi-particle dynamics. The nonlinear coupling results in transforming the original circular polarizations of the two QPs to generally elliptic ones. This means that although the initial conditions in each of the initial locations are nontrivial for only one of the functions, after the interaction both functions acquire nontrivial amplitudes for all QPs that emerge from the collision.

We consider as an initial profile the superposition of solitons with linear polarizations, one of them having only $\psi$-component, and the other only $\phi$-component. Then this initial profile is allowed to evolve according to the CNLSE system. For $\beta = 1$, $\alpha_1 = 1$, $\gamma = \Gamma = 0$, the results of the collision depend solely on the nonlinear coupling parameter $\alpha_2$ (cross-modulation parameter). We have found that for $\alpha_2 < 4$ the collision of the two initial solitons with linear polarizations results in two solitons again, but with different polarizations. The smaller soliton suffers more from the interaction and its polarization becomes elliptic.

For moderate value of the cross-modulation parameter, $\alpha_2 < 6$, we have found that an additional QP is born which propagates in the direction of the faster QP, while the initially smaller QP considerably decelerates. The initially faster QP becomes even faster. The effect of the nonlinearity is so profoundly felt that even the faster QP becomes elliptically polarized, although to a smaller extent than the slower and new-born QPs. If the initial QPs have the same phase speeds, the new-born QP is a standing soliton with circular polarization of 45°. We have observed that the energies of the initially slower QP and the new-born QP become negative after the interaction. This is due to the fact that they are steeper (with smaller support) and the potential energy (which is the stored elastic energy) becomes very negative and dominates the kinetic energy. This means that part of the energy is taken away after the interaction by the excited radiation.

Finally, we consider the case of large value of cross-modulation parameter, $\alpha_2 < 10$ and find that the dynamics changes even more radically. Now, two new QPs are born, accompanying the two initial QPs which are also radically transformed in the sense of polarization and energy. All four QPs have elliptic polarizations and negative total energies. In addition, fast forerunners with large positive (mostly kinetic) energy are born which preserves the total energy of the system, i.e., the radiation in form of forerunners evacuates positive energy leaving the ensemble of QPs with negative total energy.

## Acknowledgments

The work of CIC was supported, in part, by an ASEF/ONR Summer Faculty Fellowship. CIC gratefully acknowledges the hospitality of Dr. Stanley Chin-Bing from Stennis Space Center of Naval Research Lab and the members of his group during a summer visit.

## References

[1] F. Abdulaev, S. Darmanyan, P. Khabibullaev, Optical Solitons, Springer-Verlag, Berlin, 1993.
[2] G.P. Agrawal, Fiber-optic communication systems, second ed., Wiley, New York, 1997.
[3] N.N. Akhmediev, A. Ankiewicz, Solitons, Nonlinear Pulses and Beams, Chapman & Hall, London, 1997, p. 39.
[4] D. Anderson, Variational approach to nonlinear pulse propagation in optical fibers, Phys. Rev. A 27 (1983) 3135–3145.
[5] C.I. Christov, Gaussian elimination with pivoting for multidiagonal systems, Internal Report 4, University of Reading, 1994.
[6] C.I. Christov, S. Dost, G.A. Maugin, Inelasticity of soliton collisions in system of coupled nls equations, Physica Scripta 50 (1994) 449–454.
[7] M. Haelterman, A.P. Sheppard, The elliptically polarized fundamental vector solution of isotropic Kerr media, Phys. Lett. A 194 (1994) 191–196.
[8] M.S. Ismail, T.R. Taha, Numerical simulation of coupled nonlinear Schr¨odinger equation, Math. Comp. Simulation 56 (2001) 547–562.
[9] L.M. Kovachev, Influence of cross phase modulation and four-photon parametric mixing on the relative motion of optical pulses, Opt. Quantum Electron. 24 (1992) 1992.
[10] S.V. Manakov, On the theory of two-dimensional stationary self-focusing of electromagnetic waves, Soviet Phys. JETP 38 (1974) 248–253.
[11] M. Romagnoli, S. Trillo, S. Wabnitz, Soliton switching in nonlinear couplers, Opt. Quantum Electron. 24 (1992) S1237–S1267.
[12] W.J. Sonnier, C.I. Christov, Strong coupling of Schrödinger equations: Conservative scheme approach, Math. Comp. Simulation 69 (2005) 514–525.
[13] C. Sophocleous, D.F. Parker, Pulse collisions and polarization conversion for optical fibers, Opt. Commun. 112 (1994) 214–224.
[14] T.R. Taha, M.J. Ablovitz, Analytical and numerical aspects of certain nonlinear evolution equations. II. Numerical, Schrödinger equation, J. Comp. Phys. 55 (1984) 203–230.
[15] M.D. Todorov, C.I. Christov, Conservative scheme in complex arithmetic for coupled nonlinear Schrödinger equations, Discrete Continuous Dyn. Syst. 2007 (Suppl.) (2007) 982–992.
[16] I.M. Uzunov, R. Muschall, M. G¨olles, Y.S. Kivshar, B.A. Malomed, F. Lederer, Pulse switching in nonlinear fiber directional couplers, Phys. Rev. E 51 (1995) 2527–2537.
[17] V.E. Zakharov, A.B. Shabat, Exact theory of two-dimensional self focusing and one-dimensional self-modulation of waves in nonlinear media, Soviet Phys. JETP 34 (1972) 62–69.
[18] V.E. Zakharov, A.B. Shabat, Interaction between solitons in a stable medium, Soviet Phys. JETP 37 (1973) 823.